Photoinduced Magnetization on Mo Ion in Copper Octacyanomolybdate: An X-ray Magnetic Circular Dichroism Investigation

Marie-Anne Arrio,*,† Jérôme Long,‡ Christophe Cartier dit Moulin,‡ Anne Bachschmidt,‡ Valérie Marvaud,*,‡ Andrei Rogalev,§ Corine Mathonière,⊥ Fabrice Wilhelm,§ and Philippe Sainctavit†

Contribution from the Institut de Minéralogie et de Physique des Milieux Condensés, CNRS UMR 7590, Université Pierre et Marie Curie, 140 rue de Lourmel, 75015 Paris, France, Institut Parisien de Chimie Moléculaire, CNRS UMR7201, Université Pierre et Marie Curie, 4 place Jussieu, 75252 Paris Cedex 5, France, European Synchrotron Radiation Facility, 6 rue Jules Horowitz, BP220, 38043 Grenoble Cedex, France, and Institut de la Matière Condensée de Bordeaux, CNRS UPR 9048, Université Bordeaux, 87 avenue du Dr A. Schweitzer, 33608 Pessac, France

Received: September 10, 2009

Recently synthesized copper octacyanomolybdate molecules present interesting photomagnetic properties. Before irradiation, the molecules behave as noncoupled Cu^{II} paramagnetic ions (with central diamagnetic Mo^{IV} ion), whereas after irradiation (406 nm) they behave as superparamagnetic molecules with Cu^{II} ions coupled to the molybdenum ion. The proposed mechanism to explain these photomagnetic properties is based on the photoinduced charge transfer from Mo^{IV} ($S = 0$) to Cu^{II} ($S = 1/2$) leading to the formation of Mo^{V} ($S = 1/2$) and Cu^{I} ($S = 0$) with strong ferromagnetic coupling between Mo^{V} and the other Cu^{II} spin carriers. This paper presents X-ray magnetic circular dichroism (XMCD) measurements at the molybdenum $L_{2,3}$ edges. Two bimetallic molecules have been investigated: $[Mo(CN)_2(CN-CuL)_6]^{8+}$, L being tris(2-amino)ethylamine and $[Mo(CN)_6(CN-CuL'_2)_2]$, with L' being N,N',dimethyl ethylene diamine (labeled $MoCu_2$-Meen). In both cases, before irradiation the XMCD signal is null as expected for diamagnetic Mo^{IV} ($S = 0$). After irradiation, an XMCD signal appears, which directly demonstrates the formation of spin density on the Mo ion. After reaching room temperature, the photoinduced spectral features disappear, indicating the reversibility of the photoinduced process. In the case of $MoCu_2$-Meen, the XMCD experiments allow the observation of an X-ray-induced metastable state made of high-spin Mo^{IV} ion ($S = 1$). The application of the sum rule for isotropic spectra shows that there is no variation of the molybdenum oxidation state during the X-ray-induced magnetic process. From the Mo $L_{2,3}$ XMCD signal of the X-ray-photoexcited $MoCu_2$-Meen, we obtain an orbital magnetic moment equal to 0.13 μ_B and a spin magnetic moment equal to 1.22 μ_B at $T = 10$ K and $H = 6$ T. These results demonstrate that the Mo ion in the X-ray-photoinduced excited state of the $MoCu_2$-Meen complex is high-spin Mo^{IV} ($S = 1$).

1. Introduction

Over the past 15 years, Prussian blue analogues were used to design and synthesize new molecular-based magnets with high Curie temperatures and interesting functionalities.[1–5] One attractive issue in the field of molecular-based magnets is the development of novel opto-functionalities as extensively described in the review paper by Sato[6] (see references therein). In Prussian blue analogues, photoinduced magnetization was first observed in hexacyanometalate-based compounds, such as cobalt hexacyanoferrate, in which the electron transfer proceeds from Fe^{II} to Co^{III} by irradiation with visible light.[5c,f,g,6,7] A new family of photomagnetic cyanide compounds is born by using light-sensitive building blocks such as octacyanomolybdate or octacyanotungstate. Indeed, the photooxidation of $[Mo^{IV}(CN)_8]^{4-}$ in $[Mo^{V}(CN)_8]^{3-}$ was evidenced in the 1970s by Shirom and co-workers.[8a,b] Later Hennig and co-workers demonstrated

photoinduced electron transfer when the $[Mo^{IV}(CN)_8]^{4-}$ is associated with the Cu^{II} ion to form a donor/acceptor pair in aqueous solution.[8] The excitation of the tridimensional compounds in the intervalence band wavelength (480 nm) induces an electron transfer from Mo^{IV} to Cu^{II} ions and produces the valence isomer $Cu^{I}/[Mo^{V}(CN)_8]^{3-}$. Along this scenario, photomagnetic three-dimensional (3D) compounds were obtained.[6,9]

One of the actual challenges in the science of magnetism is the design of nanometric magnetic materials, such as nanoparticles or high-spin molecules. Combining photomagnetic properties with nanoscale particles gives rise to photomagnetic nanoparticles[10] and photomagnetic molecules.[11] In this paper, we focus on two photomagnetic molecules "$MoCu_6$-tren", $[Mo(CN)_2(CN-CuL)_6]^{8+}$, (with L = tren, tris(2-amino)ethylamine) and "$MoCu_2$-Meen" $[Mo(CN)_6(CN-CuL'_2)_2]$, (with L' = Meen, N,N',dimethyl ethylene diamine).[11] These molecules are built from the $[Mo(CN)_8]^{4-}$ entity, connected to six Cu^{II} ions for "$MoCu_6$-tren" and two Cu^{II} ions for "$MoCu_2$-Meen". Before light irradiation, the complexes behave as uncoupled paramagnetic species, as expected for isolated paramagnetic Cu^{II} (d^9, $S = 1/2$) ions surrounding a Mo^{IV} (d^2, $S = 0$) diamagnetic core. After several hours of visible light irradiation ($\lambda = 406$

* Corresponding author. E-mail address: marie-anne.arrio@impmc.jussieu.fr; valerie.marvaud@upmc.fr.
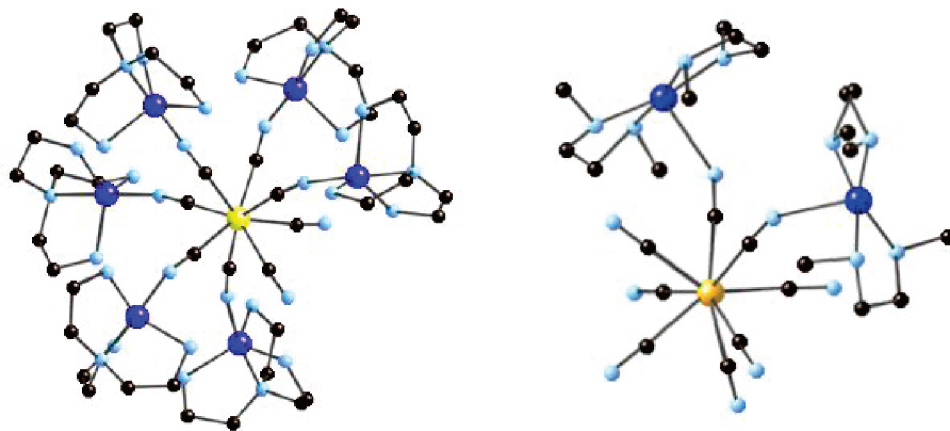† CNRS UMR 7590.
‡ CNRS UMR 7201.
§ ESRF.
⊥ CNRS UPR 9048.

Figure 1. Two photomagnetic high-spin molecules involved in this study: MoCu$_6$-tren (left) and MoCu$_2$-Meen (right) (X-ray crystallographic structures). Mo - yellow, Cu - dark blue, C - dark, N - light blue. The hydrogen atoms and solvent molecules have been omitted for clarity.

nm), an increase of the magnetization is observed. In addition, the photoinduced metastable state is persistent up to an unusually high temperature (280 K for MoCu$_6$-tren and 200 K for MoCu$_2$-Meen), and this photomagnetic effect is thermally reversible. The photomagnetic effect for MoCu$_6$-tren was explained by a photoinduced modification of the electronic structure of the Mo ion, with a charge transfer from Mo^{IV} (d^2, $S = 0$) to one Cu^{II} (d^9, $S = 1/2$) ion, leading to Mo^V (d^1, $S = 1/2$) and Cu^I (d^{10}, $S = 0$). The increase of the magnetic moment has been interpreted with ferromagnetic exchange interaction between the photoinduced Mo^V ion and the five surrounding Cu^{II} ions through cyanide bridges.[11a]

In previous works, X-ray absorption spectroscopy (XAS) was used to investigate the local structure and the electronic properties (oxidation state) of the transition metal ions involved in Prussian blue photomagnetic properties.[13,14] The chemical selectivity of this spectroscopy is a precious tool used to follow local changes induced by irradiation. For the CoFe Prussian blue analogues as well as the MnFe ones, the Fe, Co and Mn K-edge X-ray absorption fine structure (XAFS and extended XAFS or EXAFS) lead to the determination of the Fe−C, Co−N/O and Mn−N/O distances for the ground state and for the photoinduced metastable state.[13a–c,e] The low-spin Co^{III} to high-spin Co^{II} ratio was determined by X-ray absorption near edge structure (XANES) measurements at Co L$_{2,3}$ edges.[13d,f,g] The new family of Mo- and W-based photomagnetic cyanides has also been investigated by XAS at Cu and Co K edges, Mo K and L$_3$ edges, and W L$_3$ edge.[11b,14]

X-ray magnetic circular dichroism (XMCD) is an XAS dedicated to the measurement of atomic magnetic moments[15a–c] and was applied to Prussian blue analogues.[13e,15d–f] In this paper, we present XMCD measurements at Mo L$_{2,3}$ edges of the MoCu$_6$-tren and MoCu$_2$-Meen photomagnetic molecules. For the two compounds, we evidence for the first time the molybdenum spin formation during irradiation, and we can show the ferromagnetic coupling with the surrounding paramagnetic copper ions. For the MoCu$_2$-Meen complex, the XMCD experiments lead to the determination of the molybdenum oxidation state and magnetic moment in the ground state (before irradiation) and in the photoinduced state (after irradiation).

2. Experimental Section

2.1. Synthesis and Magnetic Properties. Following a rational synthetic strategy, photomagnetic high-spin molecules based on octacyanomolybdate chemistry were synthesized and entirely characterized.[11] The original MoCu$_6$-tren complex[11a] is

included in this MoCu family as well as several tri-, penta- and hepta-nuclear species, Mo^{IV}Cu$^{II}_2$, Mo^{IV}Cu$^{II}_4$, and Mo^{IV}Cu$^{II}_6$ respectively, with various external ligands for the Cu^{II} ion, counteranions, and different symmetries. XMCD measurements were performed on two of these compounds: MoCu$_6$-tren and MoCu$_2$-Meen, presented in Figure 1.[11c]

The chemical formula of the MoCu$_6$-tren compound is [Mo(CN)$_2$(CN-Cu-tren)$_6$](ClO$_4$)$_8$, where tren is tris(2-amino)-ethylamine. It is obtained as dark green crystals by addition of octacyanometalate precursor in an excess of [Cu(tren)(H$_2$O)]-(ClO$_4$)$_2$ complex, generated in situ in a H$_2$O/CH$_3$CN solution (*caution: perchlorate salt is potentially explosive*). The X-ray structure was solved, indicating that the molybdenum coordination sphere is an intermediate geometry between square anti-prism and dodecahedron. The lowest lying state in dodecahedron (D_{2d}) symmetry is d$_{x2−y2}$, and it is d$_{z2}$ in square antiprism symmetry (D_{4d}).[12] For MoCu$_6$-tren, the lowest lying d$_{z2}$ and d$_{x2−y2}$ orbitals are close in energy. The photomagnetic properties were performed in a superconducting quantum interference device (MPMS-5S Quantum Design). The irradiation was performed at 10 K under 1 T with an Ar$^+$ laser (Spectra Physics) adjusted at 406 nm. The magnetization curves were measured before and after irradiation. Before irradiation, the magnetic properties are consistent with isolated copper ions, as expected for a central diamagnetic species. After several hours of irradiation (406 nm), the magnetization curve and the thermal susceptibility dependence show a large increase with the presence of $S \geq 3$ high-spin molecules (see Figure 2).[11] This increase was previously interpreted as indicating the presence of Mo^{V}Cu^{I}Cu$^{II}_5$.[11a]

Similar results have been observed on the neutral trinuclear MoCu$_2$-Meen complex. The chemical formula of the compound is [Mo(CN)$_6$(CN-Cu-Meen$_2$)$_2$], where Meen is N,N',dimethyl ethylene diamine. It is obtained as dark blue crystals following a method similar to the MoCu$_6$-tren one, involving copper chloride and the Meen ligand.[11c] The molybdenum ion adopts an intermediate geometry between square antiprism and dodeca-hedron. Concerning the ground state, the magnetization curve at 2 K corresponds to two isolated Cu^{II} ions. After several hours of irradiation (406 nm), one observes an increase of the magnetization (see Figure 2). As for the MoCu$_6$-tren compound, these measurements were obtained with an MPMS-5S Quantum Design SQUID equipped with a Spectra Physics Ar$^+$ laser.

2.2. XMCD Measurements. The XMCD experiments at the Mo L$_{2,3}$ edges were carried out at the ESRF beamline ID12A, which is dedicated to polarization-dependent X-ray absorption
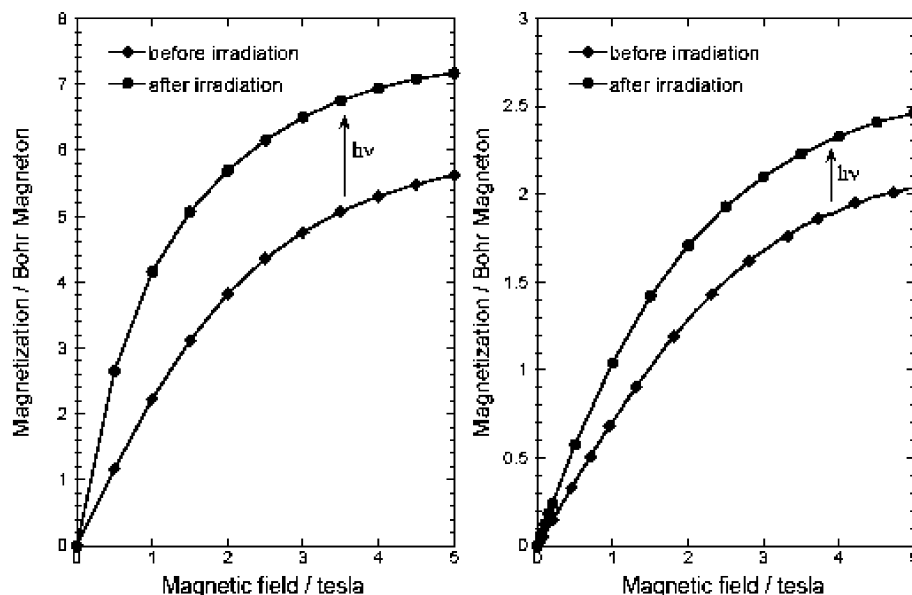
Figure 2. Magnetization curves of MoCu$_6$-tren (left) and MoCu$_2$-Meen (right) recorded by a SQUID magnetometer at $T = 2$ K: (♦) before irradiation, (●) after irradiation.

studies.[16a] The source is a helical undulator EMPHU, which emits X-ray radiation with a high polarization rate of above 97% and flexible polarization (circular left-circular right). A Si(111) double crystal setup was used as the monochromator. After the monochromator, the polarization rate drops to about 12% at the Mo L$_3$ edge (2523 eV) and 4% at the Mo L$_2$ edge (2629 eV).[16b] The circular polarization rate is particularly low at these energies. The incident beam is collimated using secondary slits located before the monochromator and closed down to 400 μm × 400 μm. The spectra are recorded using the fluorescence detection mode. The energy stability of the ID12 beamline allows an energy reproducibility better than 50 meV. In order to avoid possible radiation damages, the X-ray flux of the ESRF 4-bunch mode is severely reduced by a 25-μm thick aluminum foil inserted upstream. Compared to the conventional experimental setup, the X-ray flux is approximately reduced by a factor 10^4 on the whole L$_{2,3}$ energy range.

The powdered samples were prepared as homogeneous pellets pressed on the copper head of the sample-holder. The sample was cooled to 10 K. Because, in such an experimental setup, the visible irradiation (at 406 nm) magnetic conversion was inseparable from the X-ray induced magnetic conversion, we present results where the excited state was induced by X-ray irradiation. Several previous XAS measurements on photoswitchable systems have used X-ray-induced conversion instead of UV or visible light-induced conversion, and Yokoyama et al. even proved that X-ray-induced and photoinduced conversions were comparable.[11a,14c] We followed the X-ray-induced conversion as a function of time. We observed that the proportion of the X-ray-induced metastable state increased with time, and it reached a plateau after 6 h for both MoCu$_6$-tren and MoCu$_2$-Meen compounds.

XMCD is generally defined as the difference between the X-ray absorption cross sections measured with right and left circular polarized photons, the sample magnetization being parallel to the photon wave vector. In the electric dipole approximation, reversing the photon helicity or reversing the magnetic induction are equivalent actions.[17]

The XMCD signals were recorded by flipping the circular polarization at each energy point, with an external magnetic field applied of +6 T and then with a magnetic field in the opposite direction (−6 T). This method allows one to avoid any spurious residual XMCD signal. The absorption cross sections for a right circular polarized beam and for a magnetic field applied parallel and antiparallel to the propagation vector **k** are denoted as $\sigma^{\uparrow\uparrow}$ and $\sigma^{\uparrow\downarrow}$. In the same manner, for a left circular polarized beam, the corresponding cross sections for parallel and antiparallel fields are denoted as $\sigma^{\downarrow\downarrow}$ and $\sigma^{\downarrow\uparrow}$. The XMCD signal is obtained following $\sigma_{XMCD} = (\sigma^{\downarrow\uparrow} + \sigma^{\uparrow\downarrow})/2 - (\sigma^{\downarrow\downarrow} + \sigma^{\uparrow\uparrow})/2$. With these definitions, a negative XMCD signal at the L$_3$ edge of 3d or 4d metals corresponds to a magnetic moment pointing in the same direction as the external magnetic field. The XMCD signals presented in the paper are renormalized to 100% circular polarization light. The energy dependence of the circular polarization rate was calculated following ref 16b. By setting the monochromator at a fixed energy corresponding to a large XMCD signal, one can record a Mo-specific magnetization curve by sweeping the external magnetic field.

The Mo valence state (number of 4d electron) can be directly extracted by the use of the sum rule on the isotropic absorption spectra.[18a] The total integrated area of the isotropic spectrum (over L$_3$ and L$_2$ edges) is indeed proportional to the number of holes in the 4d shells. To apply this sum rule, the spectra were carefully normalized (see details in ref 19). The edge jump is 2 for the L$_3$ edge and 1 for the L$_2$ edge to account for the branching ratio of the continuum states.

To quantify the magnetic moment carried by the Mo ion, we applied the magneto-optic sum rules developed by Thole and Carra et al. to the XMCD spectra.[18b,c] From these sum rules, it is possible to extract the number of holes in the 4d shell, and the values of orbit and spin magnetic moments in the ground state: $\langle L_z \rangle = \langle \text{gs}|L_z|\text{gs} \rangle$ and $\langle S_z \rangle = \langle \text{gs}|S_z|\text{gs} \rangle$, where |gs⟩ is the ground state. The magnetic moment carried by the Mo absorbing atom is given by $M = -\mu_B(\langle L_z \rangle + 2\langle S_z \rangle)$, where μ_B is the Bohr magneton ($\mu_B = +5.788 \ 10^{-5}$ eV/T). The data are corrected for the self-absorption due to the fluorescence detection mode.

3. Results

3.1. MoCu$_6$-tren. *Before Irradiation.* Before irradiation, the Mo L$_3$ edge was recorded with a reduced incoming flux obtained with the instrumental configuration described in the Experi-
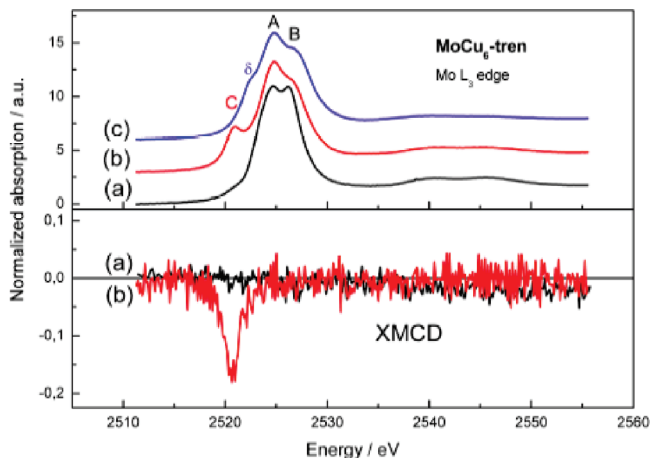
596 *J. Phys. Chem. C, Vol. 114, No. 1, 2010*

Arrio et al.

Figure 3. Absorption spectra and XMCD signals at the Mo L_3 edge of $MoCu_6$-tren recorded at $T = 10$ K and $H = \pm 6$ T: (a) before irradiation, (b) after irradiation, (c) back to 300 K after irradiation.

Figure 4. Absorption spectra and XMCD signals at the Mo L_3 edge of $MoCu_2$-Meen recorded at $T = 10$ K and $H = \pm 6$ T: (a) before irradiation, (b) after irradiation, (c) back to 300 K after irradiation.

mental Section. Figure 3 shows the absorption and XMCD spectra at the Mo L_3 edge recorded at 10 K. The absorption spectrum presents two well-resolved peaks at 2524.66 eV (peak noted A) and 2526.12 eV (peak noted B). These structures are due to the cubic part of the crystal field.[21b] Previously published papers on Mo(IV) $L_{2,3}$ edges concern oxides, therefore comparisons cannot be done. As expected for a diamagnetic Mo^{IV} ion, no XMCD signal was detected.

After Irradiation at 10 K. The compound was irradiated with the X-ray beam for 6 h. Figure 3 shows the absorption and XMCD signal recorded at 10 K and 6 T. One can observe the changes in the absorption spectra: a structure appears at low energy (peak C at 2521.00 eV), and there is almost no energy shift of peak A (2524.80 eV), whereas peak B (2526.65 eV) becomes a shoulder. An XMCD signal appears at the energy of the new peak C, and it is negative at the L_3 edge. This indicates without ambiguity that the magnetic moment of Mo ions is parallel to the external magnetic field as would be expected for ferromagnetic coupling between the central Mo ion and the outer Cu ions. Figure 3 shows the XMCD signal renormalized to 100% circular polarization. The intensity of the signal is 8% of the L_3 continuum edge jump. The same measurements were performed at the L_2 edge where the circular polarization rate is 3 times smaller than at the L_3 edge. A simple estimation shows that the experimental XMCD signal at L_2 edge prior to circular polarization renormalization cannot be expected to be larger than 0.5% of the L_2 continuum edge jump. It is found to be in the noise level of the particular low flux configuration that we adopted to avoid radiation damages.

After Annealing at 300 K (Thermal Relaxation). The compound was heated back to 300 K, and the absorption spectrum recorded at 300 K is shown in Figure 3c. We observed a partial reversibility of the phenomenon: Peak C is the characteristic feature of the molybdenum paramagnetic metastable state, and it completely disappears at 300 K. Peaks A (2524.75 eV) and B (2526.75 eV) are partially back to their initial intensity before irradiation. The main difference between spectra before irradiation and after thermal relaxation is the presence of a new shoulder δ (2522.45 eV) that we attribute to phases induced by possible radiation damages. These radiation damage phases are responsible for spectral broadening. To our knowledge, this is the first time that an XAS or XMCD study proves that an X-ray-induced excited state can relax to its original state after heating to room temperature.
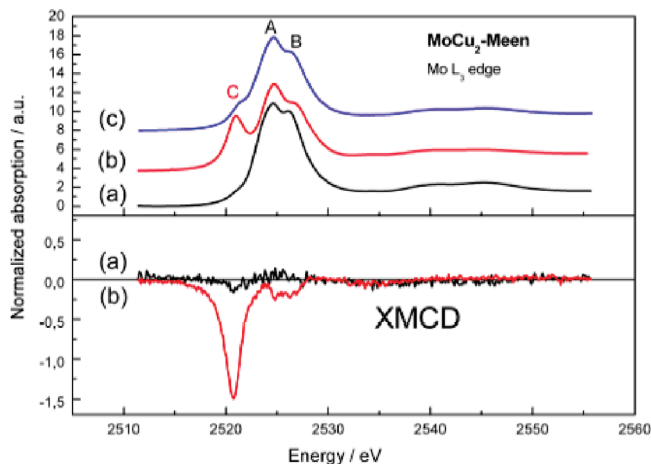
The spin change located on Mo was clearly observed with our XMCD measurements. At low temperature before irradiation, the Mo ion is in a diamagnetic state. After X-ray irradiation, one observes a partial conversion to a Mo paramagnetic metastable state. This is the direct confirmation that the photomagnetism of $MoCu_6$-tren involves the molybdenum ion. A more quantitative analysis of the XMCD data is not possible because of the very partial conversion rate in the present experimental setup.

3.2. $MoCu_2$-Meen. From the preceding $MoCu_6$-tren XMCD measurements, we directly evidenced that paramagnetic molybdenum is engaged in the photomagnetic process. We then turn toward the $MoCu_2$-Meen compound. Compared to $MoCu_6$-tren, $MoCu_2$-Meen is more favorable for XAS because the molybdenum weight concentration is roughly twice larger. The Mo $L_{2,3}$ edges and the XMCD signal for the $MoCu_2$-Meen compound were measured at 10 K and 6 T before and after 6 h of X-ray irradiation. Before irradiation, the absorption spectrum is similar to the $MoCu_6$-tren one (Figure 3a) with two peaks A (2524.62 eV) and B (2526.10 eV). The small differences in the relative intensities of the A and B peaks are probably due to the different Mo environments in $MoCu_2$-Meen and $MoCu_6$-tren. No XMCD signal is observed, as shown in Figure 4a.

XAS spectra and XMCD signal after a 6 h X-ray irradiation are presented in Figure 4b. Peak A remains at almost the same energy (2524.70 eV) as before irradiation, whereas peak B transforms into a shoulder with average energy of 2526.70 eV. As already observed for $MoCu_6$-tren, a peak C appears at low energy (2521.00 eV) on the XAS spectrum, and a large negative XMCD signal is pointing at the energy of peak C. The sign of the XMCD signal indicates ferromagnetic coupling between Mo and Cu ions as in the case of $MoCu_6$-tren. Peak C is around twice more intense for $MoCu_2$-Meen than for $MoCu_6$-tren, and the XMCD signal is also much larger. As for $MoCu_6$-tren, a partial reversibility of the process toward the initial state was observed after heating the sample at 300 K (Figure 4c). Peak C almost completely disappears, and the XAS spectrum presents only a small shoulder at 2521.20 eV. The energies of peaks A (2524.70 eV) and B (2526.50 eV) are almost the same as before irradiation, and the ratio of peak B over peak A is 6% less than before irradiation. These experiments show that molybdenum is in diamagnetic state before irradiation, and that the X-ray irradiation induces the apparition of spin density on molybdenum ion. Comparison between panels a and c of Figure 4 shows that the X-ray photoinduced process is almost reversible.
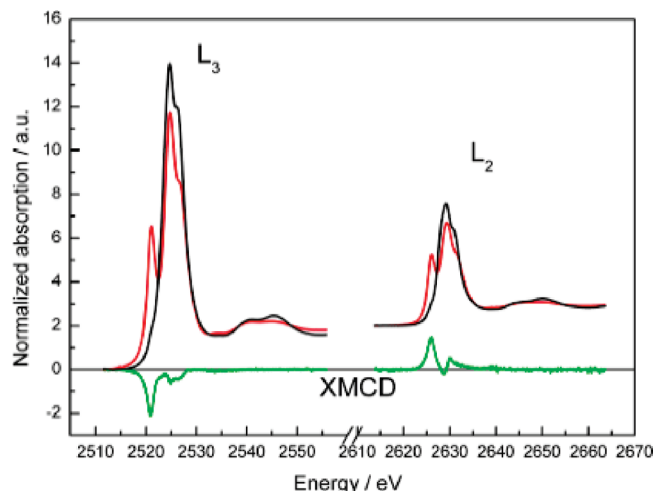
Photomagnetization on Mo in Cu Octacyanomolybdates

J. Phys. Chem. C, Vol. 114, No. 1, 2010 **597**

Figure 5. X-ray absorption spectra at the Mo L_3 and L_2 edges of MoCu$_2$-Meen recorded at $T = 10$ K and $H = \pm 6$ T. Black solid line: isotropic spectra before irradiation. Red solid line: isotropic spectra after irradiation. Green solid line: Normalized XMCD signal after irradiation.

Oxidation State of the Excited Mo. It is essential to assess the valence state of Mo in the photomagnetic phase. Finding the valence state thanks to the $L_{2,3}$ spectral features has been very helpful to follow the oxidation of Ru^{II} into Ru^{III}.[21a] It can nevertheless prove to be difficult for the $L_{2,3}$ edges of other 4d elements, as can be seen from Figure 4 in ref 20b where theoretical spectra of Mo^V and Mo^{IV} in octahedral symmetry have similar spectral features, indicating that elaborate spectral analysis is needed. The number of 4d electrons and thus the Mo valence state can be extracted by the use of the sum rule on the isotropic absorption spectra.[18a] The upper part of Figure 5 shows the isotropic spectra of MoCu$_2$-Meen at the $L_{2,3}$ edges recorded before and after irradiation. To apply the sum rule, the spectra were corrected from self-absorption effect due to the fluorescence detection.[20] The spectra were then carefully normalized (see details in ref 19). The edge jump is set to 2 for the L_3 edge and 1 for the L_2 edge to account for the branching ratio of the continuum states. The features at 2540 and 2546 eV are "so-called" shape resonance that can be simply interpreted with the Natoli's rule, as illustrated in ref 21a. The rule states that the energy of a resonance scales as the inverse of the square of a specific distance that is associated to the photoelectron scattering process. The absence of energy displacement for the two resonances tends to imply that the average medium range order (≈ 8 Å around the Mo ion) does not change during the photomagnetic conversion but for some angular reorganization.

In the hypothesis of the transformation of Mo^{IV} (number of 4d holes = 8) into Mo^V (number of 4d holes = 9) the integral of the spectra should increase in the ratio $9/8 = 1.125$. We find that the integrals of the isotropic spectra are constant before and after irradiation (the calculated ratio is found equal to 0.99 close to 1). This indicates that the number of holes (and thus the number of electrons) does not change during the X-ray-induced photoexcitation process. We conclude that there is no change in the oxidation state of the Mo ions during the X-ray photoexcitation. The relation between the chemical shift and the oxidation state has been studied in a series of papers dealing with the $L_{2,3}$ edges of 4d transition elements. It has been found that there exists a linear relation between the 4d occupation number and the chemical shift due to a one-electron oxidation.[21b] This rule that was first derived for Mo ions, was found to be

satisfied experimentally by Ruthenium $L_{2,3}$ edges during the oxidation of Ru^{IV} into Ru^V.[21c] This well-established rule states that the chemical shift for the oxidation of a Mo^{IV} ion into a Mo^V ion would be 0.8 eV. Such an energy shift is clearly absent in the Mo spectra before and after photomagnetic conversion, thus confirming that the valence state of Mo ion in the observed photomagnetic phase is likely to be Mo^{IV}. The only way to explain the existence of spin density evidenced by the XMCD signal is to suppose the formation of centered high-spin Mo^{IV} ($S = 1$) entities. In such hypothesis, the X-ray photoinduced species would be Mo$^{IV}_{HS}$Cu$^{II}_2$-Meen ($S = 2$).

Spin and Orbit Magnetic Moments of the Photoexcited Mo. The hypothesis of high-spin Mo^{IV} in the X-ray photoinduced metastable state can be confirmed by the application of the magneto-optic sum rules formula to XAS and XMCD spectra which lead to the determination of the spin and orbit magnetic moments through the integrated areas of the isotropic XAS and the XMCD signals at L_3 and L_2 edges.[18] The fluorescence-corrected and normalized isotropic spectra and XMCD spectra at Mo $L_{2,3}$ edges are reported in Figure 5 for MoCu$_2$-Meen after irradiation. The XMCD signal is for 100% circular polarized light. Applying the sum rules, one gets for Mo an orbital magnetic moment $M_L = -\mu_B\langle L_z\rangle = +0.13\ \mu_B$ and a spin magnetic moment $M_S = -g\mu_B\langle S_z\rangle = +1.22\ \mu_B$ in the hypothesis of Mo^{IV} ion (eight holes in 4d orbitals).[22] This value is compared to the calculated magnetization curves (see Figure 6) in the two hypotheses for the photoexcited state of the MoCu$_2$-Meen molecule: Cu^{II}−Mo^V−Cu^I (charge transfer from Mo to Cu with change of oxidation state), Cu^{II}−Mo^{IV}−Cu^{II} (high-spin Mo^{IV}). For comparison, we also report the calculated magnetization curve of an isolated Mo^V ion. The theoretical curves are calculated using Brillouin functions with $T = 10$ K, $g = 2$, $S = 1$ for Cu^{II}−Mo^V−Cu^I, $S = 2$ for Cu^{II}−Mo^{IV}−Cu^{II} and $S = 1/2$ for Mo^V. Figure 6b shows the theoretical magnetization curves for one molybdenum ion per molecule. By setting the X-ray monochromator at 2420.90 eV (maximum XMCD at peak C) and recording the intensity of the XMCD signal as a function of the external magnetic field, we have measured a Mo-specific magnetization curve. This Mo-specific magnetization curve is reported in Figure 6b and fits fairly well with the calculated one for Cu^{II}−Mo^{IV}−Cu^{II} hypothesis ($S = 2$).

The magnetic moment measured by XMCD is too high to be attributed to Mo^V. The value is close to the one calculated for a high-spin Mo^{IV} ion in ferromagnetic interaction with two Cu^{II} ions. Thus the XMCD measurements demonstrate the formation of high-spin Mo^{IV} ($S = 1$) in the X-ray-photoinduced excited state of MoCu$_2$-Meen.

4. Discussion

Up to now, the photomagnetic properties of octacyanomolybdate-based molecules are explained by a charge transfer from Mo^{IV} to one Cu^{II} ion, leading to Mo^V ($S = 1/2$) induced by a wavelength centered on the intervalence band (406 nm) with ferromagnetic exchange with Cu^{II} ions.[11a] Under more energetic irradiation, our results on MoCu$_2$-Meen indicate that other levels should be taken into consideration. Despite the low circular polarization rate delivered by the monochromator, we have been able to measure XMCD signals for the two compounds. Our results directly confirm that paramagnetic molybdenum is engaged in the photomagnetic process. Despite the low intensity expected for the XMCD signal, we obtained high-quality data for the MoCu$_2$-Meen compound. The analysis of the Mo $L_{2,3}$ edges clearly evidences that there is no variation of the 4d number of holes during the photoexcitation process so that there
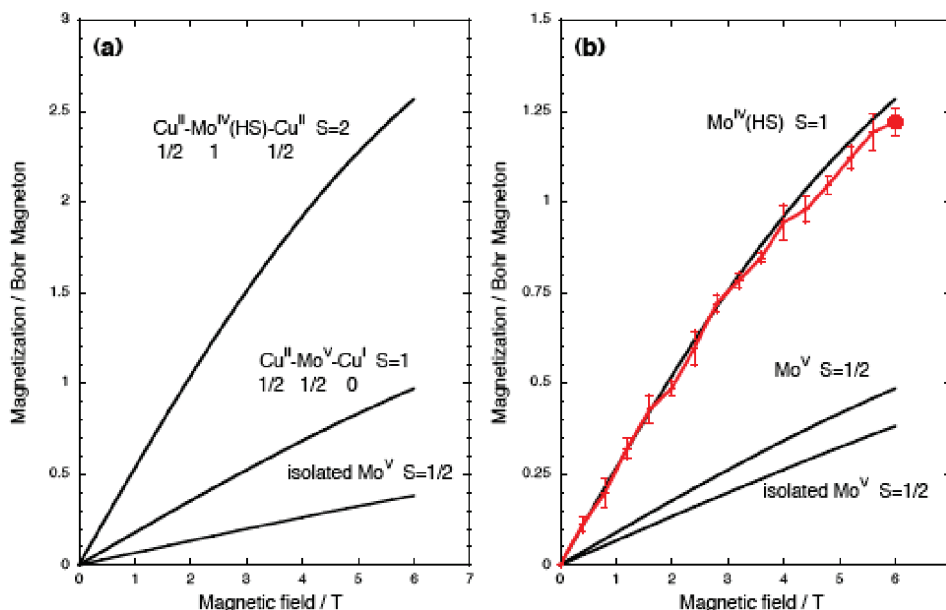
Figure 6. (a) Theoretical spin magnetization of ferromagnetically coupled Cu^{II}–$Mo^{IV}(HS)$–Cu^{II} ($S = 2$), Cu^{II}–Mo^{V}–Cu^{I} ($S = 1$) systems and isolated Mo^{V} ($S = 1/2$), at $T = 10$ K. Magnetizations are given in Bohr magneton per molecular system. (b) Theoretical spin magnetization of molybdenum ion in these systems at $T = 10$ K (the magnetization is given in Bohr magneton per molybdenum ion). The point (●) represents the Mo spin magnetic moment obtained by XMCD measurements. The red curve is the experimental Mo specific magnetization curve. The error bars are the standard deviations associated with a series of four measurements.

would be no effect of the X-rays on the oxidation state. The application of the sum rules to the XMCD spectrum yields a large magnetic moment per Mo ion in the photoexcited state ($M_S = 1.22$ μ_B and $M_L = 0.13$ μ_B per Mo ion). This value is very close to the one expected for a high-spin Mo^{IV} ion in ferromagnetic interaction with two Cu^{II} ions at 10K and 6 T. As a comparison, the expected value for Mo^{V} in ferromagnetic interaction with one Cu^{II} ion would be more than twice smaller. Thus, the XMCD results confirm the presence of an X-ray-photoinduced excited state based on high-spin Mo^{IV} ($S = 1$). In such hypothesis, the X-ray-photoinduced species would be $Mo^{IV}_{HS}Cu^{II}_2$-Meen (ferromagnetic ground state $S = 2$). We suggest in Figure 7 that the X-ray irradiation generates a singlet, and this can allow rapid singlet–triplet interconversion, leading to metastable compounds based on high-spin molybdenum, Mo^{IV} ($S = 1$). The energy difference between ground state (a) and excited states (b) or (c) is a few electron-volts. During the relaxation of the photoabsorption process (filling of the 2p Mo core hole), a huge amount of secondary electrons is created with kinetic energies between 2 and 10 eV. The absorption of these secondary electrons then triggers the transitions between ground state (a) and excited states (b) or (c). The geometry of the molybdenum (intermediate between square antiprism and dodecahedron) might explain the formation and the stability of the low-lying triplet excited state, considering that such geometry allows a triplet state even in the ground state (d_{z^2} and $d_{x^2-y^2}$ orbitals being close in energy). The peak C appearing in the Mo $L_{2,3}$ edges spectrum of the photexcited compounds (see Figure 3 and 4) would thus be roughly explained by a supplementary transition associated with the hole created in the lowest occupied orbital.

For MoCu$_6$-tren, we could apply the sum rule for the number of holes, and we find that the integrals of the isotropic spectra are constant before and after irradiation (the calculated ratio is found equal to 0.99_8 close to 1). This would indicate that Mo in MoCu$_6$-tren remains tetravalent. XMCD at the L_2 edge was too small to be measured so that spin and orbit magnetic moment could not be determined by spin and orbit sum rules and then
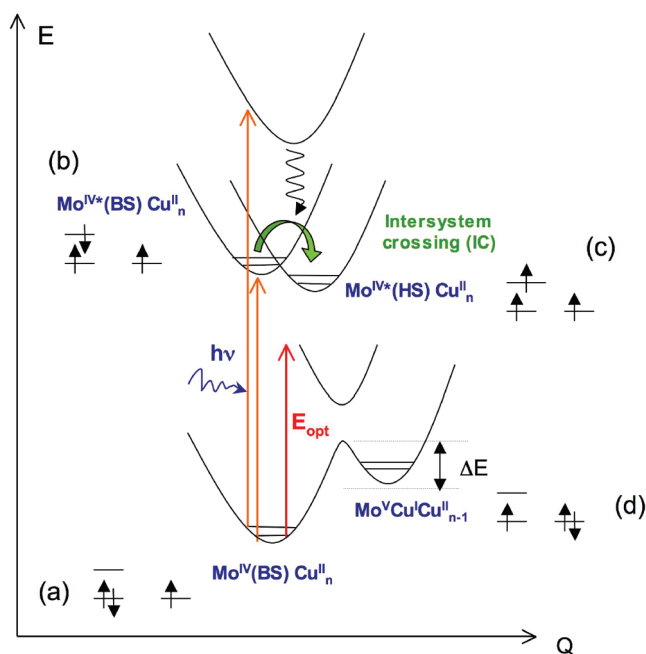

Figure 7. Suggested mechanism for the photoinduced electron transfer according to the wavelength of the irradiation: E_{opt} (406 nm) versus $h\nu$ (X-ray irradiation) correlated to the occupation of orbitals for Mo and one Cu involved in the process at (a) the ground state, (b) the lowest energy singlet excited state, (c) the lowest energy triplet excited state, and (d) the lowest energy charge-transfer metastable state.

the general picture for the excited state in MoCu$_6$-tren is not as clear as for MoCu$_2$-Meen.

5. Conclusion

Recent achievements were obtained in the field of photomagnetic high-spin molecules of potential interest for the molecular storage of information. The XMCD experiments performed on two photoactive MoCu complexes directly demonstrate for the first time the photoinduced generation of

Photomagnetization on Mo in Cu Octacyanomolybdates

J. Phys. Chem. C, Vol. 114, No. 1, 2010 **599**

spin density on the Mo core. Moreover, the analysis of XAS and XMCD spectra of the photoexcited MoCu$_2$-Meen complex has established the formation of a high-spin triplet Mo^{IV} metastable state induced by the X-ray beam. No Mo^{IV} to Mo^V transformation has been observed. Despite partial irradiation damage, the photoinduced process is mainly reversible after heating above 300 K. It should be stressed that the presence of high-spin Mo^{IV} species was established by two independent methods: the sum rule on the number of holes, and the magneto-optical sum rules. The present work might explain previously published ambiguous photomagnetic behavior of heterodimetallic molydenum complexes, and it opens a promising route toward a new family of photoswitchable compounds.

References and Notes

(1) (a) Verdaguer, M.; Bleuzen, A.; Marvaud, V.; Vaissermann, J.; Seuleiman, M.; Desplanches, C.; Scuiller, A.; Train, C.; Garde, R.; Gelly, G.; Lomenech, C.; Rosenman, I.; Veillet, P.; Cartier dit Moulin, C.; Villain, F. *Coord. Chem. Rev.* **1999**, *190−192*, 1023. (b) Hashimoto, K.; Ohkoshi, S. *Philos. Trans. R. Soc. London, Ser. A* **1999**, *357*, 2977. (c) Mallah, T.; Marvilliers, A.; Rivière, E. *Philos. Trans. R. Soc. London, Ser. A* **1999**, *357*, 3139. (d) Miller, J. S. *MRS Bull.* **2000**, *25*, 60. (e) Verdaguer, M.; Galvez, N.; Garde, R.; Desplanches, C. *Electrochem. Soc. Interface* **2002**, *11*, 28. (f) Ohkoshi, S.; Hashimoto, K. *Electrochem. Soc. Interface* **2002**, *11*, 34.

(2) (a) Mallah, T.; Thiébaut, S.; Verdaguer, M.; Veillet, P. *Science* **1993**, *262*, 1554. (b) Ferlay, S.; Mallah, T.; Ouahès, R.; Veillet, P.; Verdaguer, M. *Nature* **1995**, *378*, 701. (c) Holmes, S. M.; Girolami, G. S. *J. Am. Chem. Soc.* **1999**, *121*, 5593. (d) Hatlevik, Ø.; Buschmann, W. E.; Zhang, J.; Manson, J. L.; Miller, J. S. *Adv. Mater.* **1999**, *11*, 914. (e) Ohkoshi, S.; Mizuno, M.; Hung, G. J.; Hashimoto, K. *J. Phys. Chem. B* **2000**, *104*, 9365.

(3) (a) Ohkoshi, S.; Arai, K.; Sato, Y.; Hashimoto, K. *Nat. Mater.* **2004**, *3*, 857. (b) Ohkoshi, S.; Abe, Y.; Fujishima, A.; Hashimoto, K. *Phys. Rev. Lett.* **1999**, *82*, 1285.

(4) (a) Margadonna, S.; Prassides, K.; Fitch, A. N. *J. Am. Chem. Soc.* **2004**, *126*, 15390. (b) Margadonna, S.; Prassides, K.; Fitch, A. N. *Angew. Chem., Int. Ed.* **2004**, *43*, 6316. (c) Coronado, E.; Giménez-López, M. C.; Levchenko, G.; Romero, F. M.; García-Baonza, V.; Milner, A.; Paz-Pasternak, M. *J. Am. Chem. Soc.* **2005**, *127*, 4580. (d) Kaye, S. S.; Long, J. R. *J. Am. Chem. Soc.* **2005**, *127*, 6506. (e) Catala, L.; Gacoin, T.; Boilot, J.-P.; Rivière, E.; Paulsen, C.; Lhotel, E.; Mallah, T. *Adv. Mater.* **2003**, *15*, 826. (f) Kosaka, W.; Nomura, K.; Hashimoto, K.; Ohkoshi, S. *J. Am. Chem. Soc.* **2005**, *127*, 8590. (g) Nuida, T.; Matsuda, T.; Tokoro, H.; Sakurai, S.; Hashimoto, K.; Ohkoshi, S. *J. Am. Chem. Soc.* **2005**, *127*, 11604.

(5) (a) Ohkoshi, S.; Hashimoto, K. *J. Photochem. Photobiol. C* **2001**, *2*, 71. (b) Dei, A. *Angew. Chem., Int. Ed.* **2005**, *44*, 1160. (c) Sato, O.; Iyoda, T.; Fujishima, A.; Hashimoto, K. *Science* **1996**, *272*, 704. (d) Ohkoshi, S.; Yorozu, S.; Sato, O.; Iyoda, T.; Fujishima, A.; Hashimoto, K. *Appl. Phys. Lett.* **1997**, *70*, 1040. (e) Ohkoshi, S.; Einaga, Y.; Fujishima, A.; Hashimoto, K. *J. Electroanal. Chem.* **1999**, *473*, 245. (f) Pejakoviæ, D. A.; Manson, J. L.; Miller, J. S.; Epstein, A. *J. Phys. Rev. Lett.* **2000**, *85*, 1994. (g) Varret, F.; Goujon, A.; Boukheddaden, K.; Noguès, M.; Bleuzen, A.; Verdaguer, M. *Mol. Cryst. Liq. Cryst.* **2002**, *379*, 333. (h) Tokoro, H.; Ohkoshi, S.; Hashimoto, K. *Appl. Phys. Lett.* **2003**, *82*, 1245. (i) Arimoto, Y.; Ohkoshi, S.; Zhong, Z. J.; Seino, H.; Mizobe, Y.; Hashimoto, K. *J. Am. Chem. Soc.* **2003**, *125*, 9240. (j) Gawali-Salunke, S.; Varret, F.; Maurin, I.; Enachescu, C.; Malarova, M.; Boukheddaden, K.; Codjovi, E.; Tokoro, H.; Ohkoshi, S.; Hashimoto, K. *J. Phys. Chem. B* **2005**, *109*, 8251.

(6) Sato, O. *J. Photochem. Photobiol. C: Photochem. Rev.* **2004**, *5* (3), 203–223.

(7) (a) Sato, O.; Einaga, Y.; Iyoda, T.; Fujishima, A.; Hashimoto, K. *J. Electrochem. Soc.* **1997**, *144*, 11. (b) Shimamoto, N.; Ohkoshi, S.; Sato, O.; Hashimoto, K. *Inorg. Chem.* **2002**, *41*, 678. (c) Bleuzen, A.; Lomenech, C.; Escax, V.; Villain, F.; Varret, F.; Cartier dit Moulin, C.; Verdaguer, M. *J. Am. Chem. Soc.* **2000**, *122*, 6648. (d) Cartier dit Moulin, C.; Villain, F.; Bleuzen, A.; Arrio, M. A.; Sainctavit, Ph.; Lomenech, C.; Escax, V.;

Baudelet, F.; Dartyge, E.; Gallet, J. J.; Verdaguer, M. *J. Am. Chem. Soc.* **2000**, *122*, 6653.

(8) (a) Shirom, M.; Weiss, M. *J. Chem. Phys.* **1972**, *56*, 3170. (b) Shirom, M.; Siderer, Y. *J. Chem. Phys.* **1973**, *58*, 1250. (c) Hennig, H.; Rehorek, A.; Rehorek, D.; Thomas, P. *Inorg. Chim. Acta* **1984**, *86*, 41. (d) Rehorek, D.; Salvetter, J.; Hantschmann, A.; Hennig, H.; Stasicka, Z.; Chodkowska, A. *Inorg. Chim. Acta* **1979**, *37*, L471. (e) Hennig, H.; Rehorek, A.; Rehorek, D.; Thomas, P. *Inorg. Chim. Acta* **1983**, *77*, L11.

(9) (a) Ohkoshi, S.; Machida, N.; Zhong, Z. J.; Hashimoto, K. *Synth. Met.* **2001**, *122*, 523. (b) Rombaut, G.; Verelst, M.; Golhen, S.; Ouahab, L.; Mathonière, C.; Kahn, O. *Inorg. Chem.* **2001**, *40*, 1151. (c) Ohkoshi, S.; Machida, N.; Abe, Y.; Zhong, Z. J.; Hashimoto, K. *Chem. Lett.* **2001**, 312.

(10) (a) Catala, L.; Mathonière, C.; Gloter, A.; Stephan, O.; Gacoin, T.; Boilot, J. P.; Mallah, T. *Chem. Commun.* **2005**, 746. (b) Taguchi, M.; Yamada, K.; Suzuki, K.; Sato, O.; Einaga, Y. *Chem. Mater.* **2005**, *17*, 4554–4559. (c) Brinzei, D.; Catala, L.; Mathonière, C.; Wernsdorfer, W.; Gloter, A.; Stephan, O.; Mallah, T. *J. Am. Chem. Soc.* **2007**, *129* (13), 3778−3779.

(11) (a) Herrera, J.-M.; Marvaud, V.; Verdaguer, M.; Marrot, J.; Kalisz, M.; Mathonière, C. *Angew. Chem., Int. Ed.* **2004**, *43*, 5468. (b) Herrera, J. M.; Bachschmidt, A.; Villain, F.; Bleuzen, A.; Marvaud, V.; Wernsdorfer, W.; Verdaguer, M. *Phil. Trans. R. Soc. A* **2008**, *366*, 127–138. (c) Synthesis of [Mo^{IV}(CN)$_6${(μ-CN)Cu^{II}(N$_2$C$_4$H$_{12}$)$_2$}$_2$](H$_2$O)$_6$, MoCu$_2$-Me-en: A solution of copper chloride dihydrate (0.137 g 0.805 mmol) in water/acetonitrile (1:1, 10 mL) is added to a solution of Me-en (0.177 g, 2.014 mmol) in 10 mL of water/acetonitrile 1:1. The purple solution is stirred for 10 min before adding without stirring potassium octacyanomolybdate(IV) (0.100 g, 0.201 mmol) dissolved in 10 mL of water. The resulting mixture is allowed to stand for a couple of days in the dark before dark blue plates are collected. Yield = 94%. Elemental analysis for Mo(CN)$_8${Cu(N$_2$C$_4$H$_{12}$)$_2$}$_2$(H$_2$O)$_6$: C 32.32, H 6.78, N 25.13, Mo 10.76, Cu 14.25; found: C 32.49, H 6.34, N 25.07, Mo 10.56, Cu 14.08. IR (KBr) 2105 and 2121 cm^{-1} (shoulder) (CN asymmetric stretching). Crystal data for [MoCu$_2$-Meen]: Monoclinic, space group $C2/c$, a = 14.6282(4) Å, b = 16.3024(9) Å, c = 17.7687(18) Å, α = γ = 90°, β = 111.244(5)°, and V = 3949.4(5) Å^3. Z = 4, μ(MoKα) = 1.528 mm^{-1}, 19995 reflections measured, 5648 independent (R_{int} = 0.0573), 5648 observed [$I > 2\sigma(I)$], 259 refined parameters, final R indices R_1 [$I > 2\sigma(I)$] = 0.0565 and wR_2 = 0.1254.

(12) Sieklucka, B.; Podgajny, R.; Przychodzeń, P.; Korzeniak, T. *Coord. Chem. Rev.* **2005**, *249* (21−22), 2203–2221.

(13) (a) Yokoyama, T.; Ohta, T.; Sato, O.; Hashimoto, K. *Phys. Rev. B* **1998**, *58* (13), 8257–8266. (b) Yokoyama, T; Kiguchi, M.; Ohta, T.; Sato, O.; Einaga, Y.; Hashimoto, K. *Phys Rev B* **1999**, *60* (13), 9340–9346. (c) Yokoyama, T.; Tokoro, H.; Ohkoshi, S.-I.; Hashimoto, K.; Okamoto, K.; Ohta, T. *Phys. Rev. B* **2002**, *66*, 184111. (d) Cartier dit Moulin, C.; Villain, F.; Bleuzen, A.; Arrio, M.-A.; Sainctavit, Ph.; Lomenech, C.; Escax, V.; Baudelet, F.; Dartyge, E.; Gallet, J.-J.; Verdaguer, M. *J. Am. Chem. Soc.* **2000**, *122* (28), 6653–6658. (e) Champion, G.; Escax, V.; Cartier dit Moulin, C.; Bleuzen, A.; Villain, F.; Baudelet, F.; Dartyge, E.; Verdaguer, M. *J. Am. Chem. Soc.* **2001**, *123* (50), 12544–12546. (f) Escax, V.; Champion, G.; Arrio, M.-A.; Zacchigna, M.; Cartier dit Moulin, C.; Bleuzen, A. *Angew. Chem., Int. Ed.* **2005**, *44* (30), 4876–4879. (g) Cartier dit Moulin, C.; Champion, G.; Cafun, J.-D.; Arrio, M.-A.; Bleuzen, A. *Angew. Chem., Int. Ed.* **2007**, *46* (8), 1287–1289.

(14) (a) Ohkoshi, S.; Tokoro, H.; Hozumi, T.; Zhang, Y.; Hashimoto, K.; Mathonière, C.; Bord, I.; Rombaut, G.; Verelst, M.; Cartier dit Moulin, C.; Villain, F. *J. Am. Chem. Soc.* **2006**, *128* (1), 270–277. (b) Ma, X.-D.; Yokoyama, T.; Hozumi, T.; Hashimoto, K; Ohkoshi, S. *Phys. Rev. B* **2005**, *72*, 094107. (c) Yokoyama, T.; Okamoto, K.; Ohta, T.; Ohkoshi, S.; Hashimoto, K. *Phys. Rev. B* **2002**, *65*, 064438.

(15) (a) de Groot, F. M. F.; Kotani, A. *Core Level Spectroscopy of Solids*; Advances in Condensed Matter Science Series; CRC Press: Boca Raton, FL, 2008. (b) Stöhr, J. *J. Electron Spectrosc. Relat. Phenom.* **1995**, *75*, 253. (c) Stöhr, J. *J. Magn. Magn. Mater.* **1999**, *200*, 470–497. (d) Arrio, M. A.; Sainctavit, Ph.; Cartier dit Moulin, Ch.; Brouder, Ch.; de Groot, F. M. F.; Mallah, T.; Verdaguer, M. *J. Phys. Chem.* **1996**, *100*, 4679–4684. (e) Dujardin, E.; Ferlay, S.; Phan, X.; Desplanches, C.; Cartier dit Moulin, C.; Sainctavit, Ph.; Baudelet, F.; Dartyge, E.; Veillet, P.; Verdaguer, M. *J. Am. Chem. Soc.* **1998**, *120*, 11347–11352. (f) Arrio, M. A.; Scuiller, A.; Sainctavit, Ph.; Cartier dit Moulin, Ch.; Mallah, T.; Mallah, T.; Verdaguer, M. *J. Am. Chem. Soc.* **1999**, *121*, 6414–6420.

(16) (a) *ID12 Circular Polarisation Beamline*; European Synchrotron Radiation Facility: Cedex 9, France; 2006; http://www.esrf.eu/UsersAndScience/Experiments/ElectStructMagn/ID12. Accessed 06/05/2009. (b) Lefebvre, D.; Sainctavit, Ph.; Malgrange, C. *Rev. Sci. Instrum.* **1994**, *65*, 2556.

(17) Brouder, C.; Kappler, J.-P. *Magnetism and Synchrotron Radiation, Lecture Notes*, Mittelwihr, 1996, E. Beaurepaire, B. Carrière, J.-P. Kappler Eds; Les Editions de Physique: Les Ulis, France, 1997, p. 19.

(18) (a) Thole, B., T.; van der Laan, G. *Phys. Rev. A* **1988**, *38* (4), 1943–1947. (b) Thole, T.; Carra, P.; Sette, F.; van der Laan, G. *Phys. Rev. Lett.* **1992**, *68*, 1943–1946. (c) Carra, P.; Thole, B. T.; Altarelli, M.; Wang, X. *Phys. Rev. Lett.* **1993**, *70* (5), 694–967.

(19) The spectra were divided by the integrated area of the absorption spectrum after the L_3 edge (from 2532 to 2555 eV) and at the L_2 edge (from 2638 to 2664 eV). The edge jump is set from 0 to 2 at the L_3 edge and from 2 to 3 after L_2, in order to account for the branching ratio of the continuum states: the spin-orbit coupling splits the 2p core hole levels in two states corresponding to $j = l + s = 3/2$ (L_3 edge) with a 4-fold degeneracy and $j = l - s = 1/2$ (L_2 edge) with a 2-fold degeneracy. The L_3/L_2 ratio is thus equal to 2.

(20) Goulon, J.; Goulon-Ginet, C.; Cortes, R.; Dubois, J. M. *J. Phys. (Paris)* **1982**, *43*, 539–548.

(21) (a) Gawelda, W.; Johnson, M; de Groot, F. M. F.; Abela, R.; Bressler, C.; Chergui, M. *J. Am. Chem. Soc.* **2006**, *128*, 5001. (b) de Groot, F. M. F.; Hu, Z. W.; Lopez, M. F.; Kaindl, G.; Guillot, F.; Tronc, M. *J. Chem. Phys.* **1994**, *101*, 6570. (c) Hu, Z.; Golden, M. S.; Ebbinghaus, S. G.; Knupfer, M.; Fink, J.; de Groot, F. M. F.; Kaindl, G. *Chem. Phys.* **2002**, *282*, 451–463.

(22) In the hypothesis of Mo^V (nine holes in 4d orbitals), the sum rules lead to $M_S = -g\mu_B\langle S_z\rangle = +1.38\ \mu_B$ and $M_L = -\mu_B\langle L_z\rangle = +0.15\ \mu_B$.

JP9087699